

# A Memristive Model for Graphene Emitters: Hysteresis and Self-Crossing

Dmitriy V. Gorodetskiy,\* Sergey N. Shevchenko, Artem V. Gusel'nikov,  
and Aleksandr V. Okotrub

Hysteresis exhibited by current–voltage characteristics during field-emission experiments is often considered undesirable in terms of practical applications. However, this is an appealing effect for the purposes of memristive devices. A two-stage model to describe hysteretic characteristics is developed, with a particular focus on the system which includes a cathode made of a single-layered graphene sheet on a substrate. In addition to hysteresis, the current–voltage curves also display an unusual self-crossing behavior. The presented memristive model can be used for quantitative description of different hysteretic characteristics such as abrupt changes and self-crossings and for understanding and modeling the processes associated with field emission from plane graphene emitters.

## 1. Introduction

Graphene is an interesting material that combines a variety of physical and chemical properties. Its application areas are sometimes quite surprising. One possible direction of graphene research is field emission occurring at the edges of graphene sheets. Here, graphene shows some interesting features. In addition to high aspect ratio, field emission from graphene cathodes demonstrates another intriguing feature, namely, huge hysteresis in current–voltage dependences.<sup>[1–5]</sup> Hysteresis in current–voltage characteristics of field emission may be due to a variety of factors such as the emitter temperature, sorption of residual gases on the emitter's surface, and mechanical changes of the emitter's shape under the influence of an electromagnetic field.<sup>[6–10]</sup>

Hysteresis in field emission is ubiquitous (e.g., see refs. [4,11–14]). It is therefore important to develop a transparent and functional theory that would describe different hysteretic dependences

possibly exhibiting nontrivial behavior such as abrupt changes or self-crossings. In this work, experimental data were used to develop a mathematical model that qualitatively describes field emission from graphene sheets. The model describes well the hysteresis in the  $I$ – $V$  characteristic characterized by self-intersection and can be used to understand the processes accompanying electron emission by planar emitters having physical and chemical properties similar to those of graphene.

Hysteresis in current–voltage characteristics is useful for memory devices commonly referred to as memristors.<sup>[11,15,16]</sup> Memristive devices are novel elements of electric circuits, in which the relation

between output and input signals is determined by a dynamic internal state variable.<sup>[16]</sup> For definiteness, suppose there is an element with voltage  $U(t)$  (the input), current  $I(t)$  (the output), and an internal variable  $x(t)$  (to be discussed later). Then, the memory element, the memristor, is defined by the following general relations

$$I(t) = G_M(x, U, t)U(t) \quad (1)$$

$$\dot{x} = f(x, U, t) \quad (2)$$

where  $G_M$  is the conductance (also called memductance, from “memory conductance”), which depends both on the input voltage and on the internal system state; this function is the inverse of memory resistance, the memristance. The dynamics of the internal variable  $x$  is defined by function  $f$ .

It will be shown on the example of field emission from a graphene cathode that experimental results can be conveniently described by our model. In particular, both our own experimental results and those reported recently by Kleshch et al.<sup>[4]</sup> will be discussed. It is important to note that this approach can also be adapted to other systems, e.g., nanomechanical systems such as those discussed in previous studies<sup>[17–20]</sup> (see also ref. [21] and discussion in ref. [16]).

Thus, measuring current–voltage characteristics of graphene experimentally and developing a theoretical model that would be well comparable with experimental data is an important problem. In this work, we present a comprehensive study of hysteretic field emission from graphene cathodes; theoretical, technological, and experimental aspects are discussed.

Dr. D. V. Gorodetskiy, Dr. A. V. Gusel'nikov, Prof. A. V. Okotrub  
Nikolaev Institute of Inorganic Chemistry SB RAS  
Novosibirsk 630090, Russia  
E-mail: gorodetskiy@niic.nsc.ru

Dr. S. N. Shevchenko  
B. Verkin Institute for Low Temperature Physics and Engineering  
Kharkov 61103, Ukraine

Dr. S. N. Shevchenko  
V. N. Karazin Kharkov National University  
Kharkov 61022, Ukraine

 The ORCID identification number(s) for the author(s) of this article can be found under <https://doi.org/10.1002/pssb.202000020>.

DOI: 10.1002/pssb.202000020

## 2. Experimental Realization of Graphene Field Emitter

Field-emission characteristics were measured using graphene by Graphenea, CIC nanoGUNE, Spain. The graphene was synthesized by chemical vapor deposition (CVD) on a copper substrate and then transferred to a silicon substrate. A  $10 \times 10$  mm area of the silicon substrate was covered with a natural  $\text{SiO}_2$  layer.

The sample was characterized by scanning electron microscopy (SEM) on a Helios 450S system and by Raman spectroscopy on a HORIBA LabRAM HR Evolution spectrometer with an Ar<sup>+</sup> laser excitation of 514 nm. The SEM image in **Figure 1a** shows the graphene surface structure. The micrographs were taken at an accelerating voltage of  $\approx 1$  kV. As can be seen, there are minor areas of two-to-three layer graphene, which occupy less than 3% of the sample surface.

**Figure 1b** shows the graphene Raman spectrum. The laser spot diameter was about  $20 \mu\text{m}$ , and the radiation power was 1 mW. The spectrum demonstrates G and 2D bands typically of graphene. The integrated intensities of G and 2D bands have approximately equal values to confirm a presence of several well-graphitized layers of graphene on the substrate surface.

To obtain smooth graphene edges, the substrates were mechanically cut into rectangular pieces (**Figure 1c,d**). **Figure 1c** shows the SEM image of the edges of the sample after splitting. As can be seen, graphene was broken irregularly and partially protruded beyond the silicon substrate. The protruding graphene edge has a size of about  $6 \times 2 \mu\text{m}$ . The radius of curvature of the ring-shaped graphene edge is about  $0.5 \mu\text{m}$ . The side view of the sample is schematically shown in **Figure 1d**.

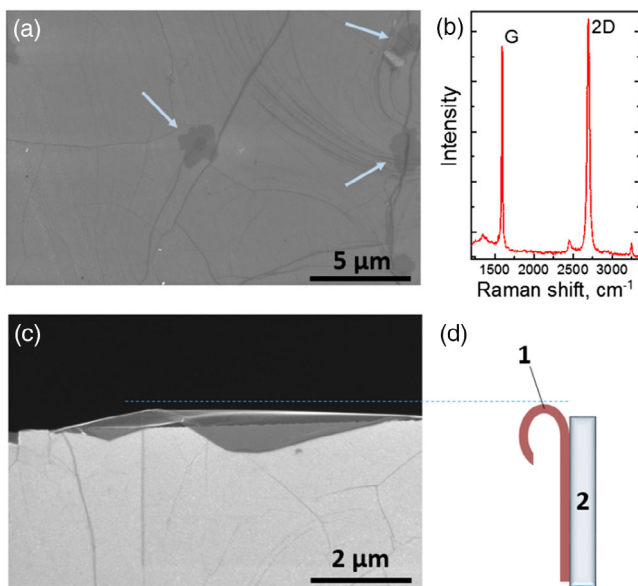


**Figure 1.** a) SEM image of the surface of a silicon substrate coated by graphene, the arrows show the regions of graphene; b) Raman spectra of graphene. c) SEM image of the edge of the silicon substrate coated with graphene, top view; d) the same shown schematically; graphene and substrate designated by digits 1 and 2, respectively, side view.

## 3. Current–Voltage Characteristics

The current–voltage characteristics were measured on our home-made setup for field-emission probing of carbon nanomaterials.<sup>[22]</sup> A half of the silicon substrate was placed in the  $10^{-5}$  Torr vacuum chamber of the installation so that its fresh cut was directed toward the anode. The cut edge of graphene was parallel to the anode surface. The measurement scheme is shown in **Figure 2a**. An excitation voltage of 0–2.5 kV in diode configuration was applied to the sample at a frequency of 5 Hz. The sensitivity of the measuring current of the field emission was of the order of nA. The distance between the sample and the anode was controlled by a micromechanical screw system and was set equal to 1 mm.

**Figure 2b** shows  $I$ – $V$  characteristics of several consecutive cycles. Note that the hysteretic curve has a self-intersection point. **Figure 2c** shows a calculated  $I$ – $V$  characteristic with a self-intersecting hysteretic curve to be discussed in Section 4.

## 4. Modeling the Self-Crossing Hysteresis

### 4.1. Two-Stage Memristive Model

Let us describe the dynamics of the internal variable  $x(t)$ . First, we assume that this value varies from 0 to 1. We also require that it switches from 0 to 1 at  $U = U_A$  as the voltage increases and back from 1 to 0 at  $U = U_B < U_A$  as the voltage decreases. Let  $r$  be the rate of this transition, then the corresponding transition time is equal to  $r^{-1}$ . These requirements result in the dependence shown in **Figure 3**, that can also be written as equation

$$\dot{x} = r\{\theta(U - U_A)\theta(1 - x) - \theta(U_B - U)\theta(x)\} \equiv f(x, U, t) \quad (3)$$

which corresponds to the second memristor relation (Equation (2)). According to ref. [4], we take  $U_A = 0.35$  kV,  $U_B = 0.05$  kV and assume that the voltage varies periodically between 0 and  $U_{\text{max}} = 0.5$  kV.

### 4.2. Hysteretic Current–Voltage Characteristics

To start with, we summarize some main features; more details can be found in the comprehensive analysis of Kleshch et al.<sup>[4]</sup> 1) The current–voltage characteristics for the blade-type graphene emitter obey the Fowler–Nordheim law (see also refs. [23–25]). 2) Strong hysteresis cannot be explained neither by absorption of residual gas atoms and molecules nor by heating. 3) Instead, it is explained by mechanical peeling of graphene sheet from the substrate. 4) The effective emission surface (proportional to the number of emitting sites) changes for the increasing voltage curve and remains virtually the same for the decreasing voltage curve. 5) The self-crossing of the hysteretic curve can be observed at high voltages. Based on these observations, a model for quantitative description of such phenomena will be developed in this section.

Let a potential difference  $U(t)$  be applied between the cathode and the anode. It causes electric field  $E = \beta U/D$ , where  $D$  is the distance between the electrodes and  $\beta$  is the field enhancement

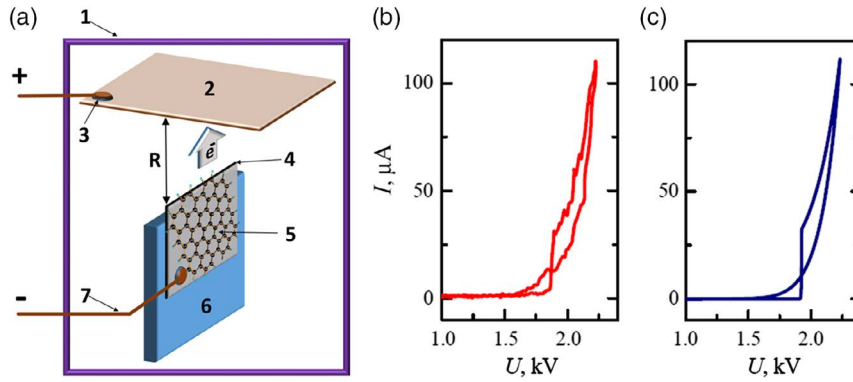


**Figure 2.** a) Schematic experimental setup for field-emission measurements: vacuum chamber of the field-emission measurement system (1), flat anode (2), positive potential contact (3), emitting edge of graphene (4), silicon substrate coated with graphene (5), mobile substrate holder (6), negative electrode contact (7). Hysteretic self-crossing of current–voltage characteristics: b) experiment and c) theory. The rapid change of the form factor and the self-crossing point are shown.

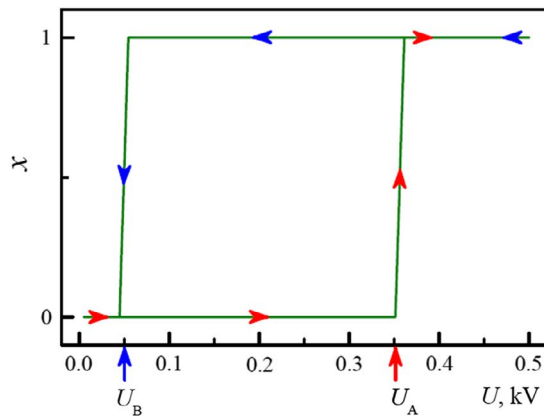


**Figure 3.** Two-stage model with a memristor internal variable  $x$  rapidly switching between two input values. For definiteness, the changes in this system are assumed to occur at  $U = U_{A,B}$ .

factor (form factor). Then, the emission current density at relatively low temperatures  $T \ll \varphi/k_B$  is described by the Fowler–Nordheim formula<sup>[26,27]</sup>

$$I(U) = AU^2 \exp\left(-\frac{B}{U}\right) \quad (4)$$

$$A = \frac{e^3}{16\pi^2 \hbar} \frac{1}{\varphi} \left(\frac{\beta}{D}\right)^2 S, \quad B = \frac{4\sqrt{2m}}{3e\hbar} \varphi^{3/2} \left(\frac{\beta}{D}\right)^{-1} \quad (5)$$

where  $e$  is the electron charge,  $m$  is the electron mass,  $\hbar$  is Planck's constant,  $k_B$  is the Boltzmann constant; the dimension of quantity  $S$  is the same as that of area and can be treated in the first approximation as the area of the emitting surface; the work function is assumed here constant and equal to  $\varphi = 4.8$  eV.

Thus, formula (4) contains two fitting parameters  $S$  and  $b = \beta/D$ . It was assumed in the experiments that the former is either constant or a slowly changing parameter, whereas the latter changes rapidly at  $U = U_{A,B}$  together with the form factor when the graphene sheet delaminates and sticks back. For simplicity, the changes of the emitting surface  $S$  will be neglected and the

variable  $x$  is assumed to describe the variation of parameter  $b$  (or form factor  $\beta$ ) so that  $x = 0$  (1) corresponds to low (high) form factor values and can be termed as high-resistance (low-resistance) states. As a result, we obtain a memristive model of field emission, which can be rewritten in the form of Equation (1) and (2) with

$$G_M(x, U) = A(x) U \exp\left(-\frac{B(x)}{U}\right) \quad (6)$$

$$A(x) = A_0(1-x) + A_1x, \quad B(x) = B_0(1-x) + B_1x \quad (7)$$

This means that the increase in the form factor (i.e., graphene sheet delamination) results in transitions from  $B(0) = B_0$  to  $B(1) = B_1 < B_0$  and from  $A_0$  to  $A_1 > A_0$ .

Alternatively, delamination of a large-area graphene sheet can be described as a continuous process whereby some part of the sheet (with a relative weight  $x$ ) is peeled off, whereas its other part (with a relative weight  $1-x$ ) remains stuck. This would result in the total conductance

$$G_M = G_{M0} + G_{M1} \equiv (1-x)A_0 U e^{-\frac{B_0}{U}} + xA_1 U e^{-\frac{B_1}{U}} \quad (8)$$

According to our calculations, the dependences furnished by this model are very similar to those of the former model (Equation (6)). Therefore, for definiteness, we will later explore the model of Equation (6). Note that in ref. [15], it was more convenient to use the model of Equation (8).

**Figure 4a** shows a strong hysteretic current–voltage cycle with the following parameters:  $A_1 = 2300$ ,  $B_1 = 0.66$ ,  $A_0 = 200$ , and  $B_0 = 5$ . We assume here that  $I$  and  $U$  are given in  $\mu\text{A}$  and kV, respectively, so that coefficients  $A_i$  and  $B_i$  are dimensionless. The switching voltage  $U_A$  has two values so that these two curves are related to two experimental results presented by Kleshch et al. in ref. [4] (Figures 3 and 5 therein, respectively).

### 4.3. Self-Crossing

The calculation results are presented in the logarithmic scale in Figure 4a. However, it is sometimes more convenient to use the linear scale (Figure 4b) for clarity reasons (cf. also the hysteresis

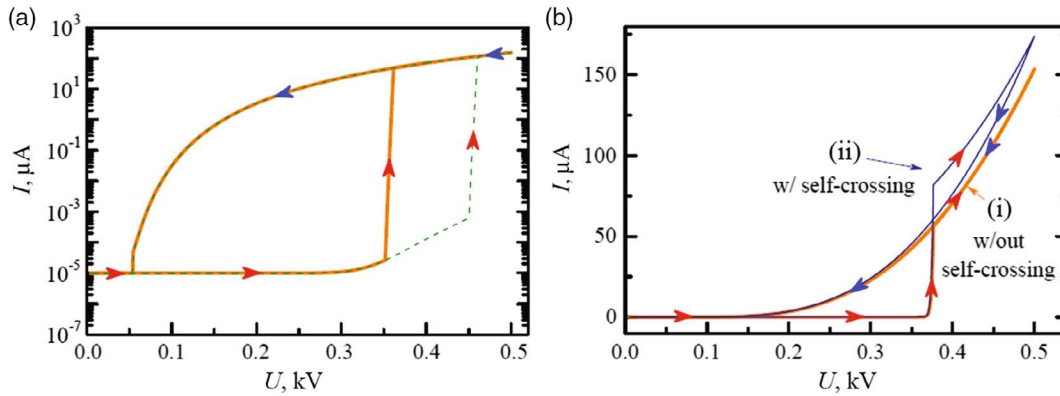


**Figure 4.** a) Hysteretic current–voltage cycles with  $U_B = 0.05$  and  $U_A = 0.35$  and  $0.45$  for thick solid and thin dashed lines, respectively. b) Current–voltage characteristics in the linear scale (thick orange line (i)) as described by the rapidly changing parameter  $x$ . A self-crossing loop appearing as a result of nonequilibrium changes caused by the effect of inertia (thin blue line (ii)).

in ref. [28]) so that the high-voltage region becomes better visible. Note that the self-crossing of hysteretic curves, which is barely visible in Figure 3 and 5 of ref. [4], is more pronounced in the linear scale.

To describe the self-crossing, we need to consider the effect of nonequilibrium. We consider here a visual model, which assumes, in addition to the previous consideration, that the peeled-off graphene sheet in the course of delamination moves at a slightly more distant position than that described by  $x = 1$  and corresponds to some  $x_M > 1$ . This happens after the voltage reaches  $U = U_A$ . **Figure 5a** shows time dependence of parameter  $x$  where time is normalized with respect to the driving frequency  $\nu$  ( $\tau = \nu \times t$ ). The second stage starts at  $\tau_A$  and proceeds until  $\tau_A + \delta$ , where  $\delta = \nu \times r^{-1}$ . Then, there is a relaxation stage that

proceeds with rate  $\Gamma$  and is described by  $\gamma = \Gamma/\nu$ . Finally,  $x$  rapidly drops from 1 to 0 at  $\tau = \tau_B$  (when  $U = U_B$ ) to describe graphene sheet sticking back to the substrate. We believe that this model provides clear physical interpretation of most relevant and nontrivial features of hysteretic curves; we avoided overcomplicating in other possible changes during the variation of the voltage. Furthermore, Figure 5b shows the dependence of parameter  $x$  on the voltage, where the values  $U_A$  and  $U_B$  are defined in accordance with the experiment, as described later. By comparing Figure 5b with Figure 3, one can explicitly see a self-crossing loop appearing in the model.

Let us now consider the model shown in Figure 2c, having in mind to compare this with our in-home experiment. This theoretical graph was plotted according to Equation (6),

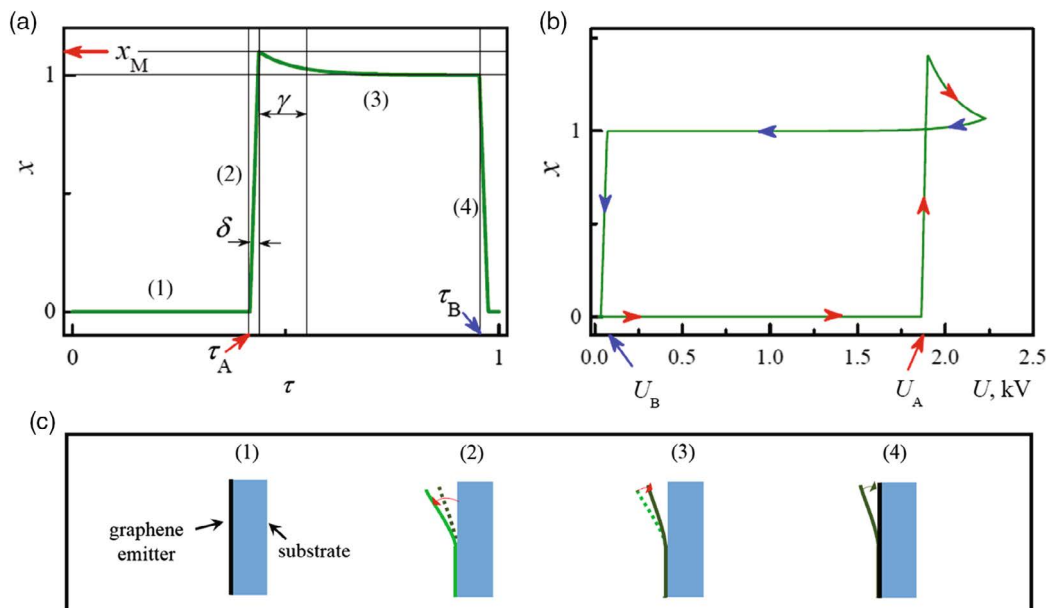


**Figure 5.** a) Four-stage model for parameter  $x$ :  $x = 0$  (graphene sheet is attached to the substrate) (1);  $x$  rapidly switches from 0 to 1 and to a still higher value  $x_M > 1$  due to inertia (graphene is peeled off from the substrate, the form factor is abruptly increased) (2); relaxation to 1 (graphene sheet returns to its equilibrium delaminated position) (3);  $x$  rapidly switches from 1 to 0 (as the voltage decreases, the graphene sheet sticks back to the substrate) (4). b) Voltage dependence of parameter  $x$  in the model with a self-crossing point. c) The above four stages are shown schematically.

and the dependence  $x = x(U(\tau))$  was taken from Figure 5. The following parameters were used:  $A_1 = 1000$ ,  $B_1 = 25$ ,  $A_0 = A_1/9$ , and  $B_0 = 3B_1$  (corresponding to a threefold increase in the form-factor, cf. Equation (5));  $U_A = 1.86$  kV,  $U_B = 0.05$  kV,  $x_M = 1.05$ ,  $r = 0.36$  kHz,  $\Gamma = 0.06$  kHz. Similarly, Figure 4b shows a thin blue line which is not only changing abruptly but also contains a self-crossing point due to the nonequilibrium described by  $x_M > 1$  (more specifically,  $x_M$  was taken to be equal to 1.03).

## 5. Conclusion

A model describing hysteretic current–voltage cycles was developed for the field emission from a graphene cathode. The mechanical motion of graphene being peeled off from the substrate was described in terms of a two-stage memristive model that was shown useful compared with realistic experiments. In contrast, such layout may be useful for memristive applications. Having small operation frequencies and being reliably realized and controlled, they can be used to model their more practical counterparts, fast and small nanoscale memristors. Some possible applications to the realization of logic operations are discussed elsewhere.<sup>[15]</sup>

## Acknowledgements

This work was supported by the Russian Science Foundation (grant no. 15-13-20021).

## Conflict of Interest

The authors declare no conflict of interest.

## Keywords

field emission, graphene, memristors

Received: January 13, 2020  
Revised: March 11, 2020  
Published online: April 6, 2020

- [1] K. S. Novoselov, A. K. Geim, S. V. Morozov, D. Jiang, Y. Zhang, S. V. Dubonos, I. V. Grigorieva, A. A. Firsov, *Science* **2006**, 306, 666.  
[2] L. Chen, H. Yu, J. Zhong, J. Wu, W. Su, *J. Alloys Compd.* **2018**, 749, 60.  
[3] S. Yu, R. Tang, K. Zhang, S. Wu, X. Yang, W. Wu, Y. Chen, Y. Shen, X. Zhang, J. Qian, Y. Song, Z. Sun, *Vacuum* **2019**, 168, 108817.

- [4] V. I. Kleshch, D. A. Bandurin, A. S. Orekhov, S. T. Purcell, A. N. Obraztsov, *Appl. Surf. Sci.* **2015**, 357, 1967.  
[5] Y. S. Ang, S.-J. Liang, L. K. Ang, *MRS Bull.* **2017**, 42, 506.  
[6] E. O. Popov, A. G. Kolosko, S. V. Filippov, P. A. Romanov, E. I. Terukov, A. V. Shchegolkov, A. G. Tkachev, *Appl. Surf. Sci.* **2017**, 424, 239.  
[7] A. V. Okotrub, A. G. Kurennya, A. V. Gusel'nikov, A. G. Kudashov, L. G. Bulusheva, A. S. Berdinskii, Y.A. Ivanova, D. K. Ivanov, E. A. Strel'tsov, D. Fink, A. V. Petrov, E. K. Belonogov, *Nanotechnol. Russ.* **2009**, 4, 627.  
[8] J. Chen, J. Li, J. Yang, X. Yan, B.-K. Tay, Q. Xue, *Appl. Phys. Lett.* **2011**, 99, 173104.  
[9] A. Kumar, S. Khan, M. Zulfequar, M. Husain, *Appl. Surf. Sci.* **2017**, 402, 161.  
[10] L. Chen, H. Yu, J. Zhong, L. Song, J. Wu, W. Su, *Mater. Sci. Eng. B* **2017**, 220, 44.  
[11] D. V. Gorodetskiy, A. V. Gusel'nikov, S. N. Shevchenko, M. A. Kanygin, A. V. Okotrub, Y. V. Pershin, *J. Nanophotonics* **2016**, 10, 012524.  
[12] M. Sveningsson, K. Hansen, K. Svensson, E. Olsson, E. E. B. Campbell, *Phys. Rev. B* **2005**, 72, 085429.  
[13] Y. V. Fedoseeva, L. G. Bulusheva, A. V. Okotrub, M. A. Kanygin, D. V. Gorodetskiy, I. P. Asanov, D. V. Vyalikh, A. P. Puzyr, V. S. Bondar, *Sci. Rep.* **2015**, 5, 9379.  
[14] S. V. Filippov, E. O. Popov, A. G. Kolosko, E. I. Terukov, P. A. Romanov, *J. Phys. Conf. Ser.* **2016**, 741, 012029.  
[15] Y. V. Pershin, S. N. Shevchenko, *Nanotechnology* **2017**, 28, 075204.  
[16] Y. V. Pershin, M. Di Ventra, *Adv. Phys.* **2011**, 60, 145.  
[17] S. Axelsson, E. E. B. Campbell, L. M. Jonsson, J. Kinaret, S. W. Lee, Y. W. Park, M. Sveningsson, *New J. Phys.* **2005**, 7, 245.  
[18] T. Barois, S. Perisanu, P. Vincent, S. T. Purcell, A. Ayari, *Phys. Rev. B* **2013**, 88, 195428.  
[19] J. Sun, M. E. Schmidt, M. Muruganathan, H. M. H. Chong, H. Mizuta, *Nanoscale* **2016**, 8, 6659.  
[20] R. D. Yamaletdinov, O. V. Ivakhnenko, O. V. Sedelnikova, S. N. Shevchenko, Y. V. Pershin, *Sci. Rep.* **2018**, 8, 3566.  
[21] H. Nieminen, V. Ermolov, K. Nybergh, S. Silanto, T. Ryhanen, *J. Micromech. Microeng.* **2002**, 12, 177.  
[22] A. V. Okotrub, L. G. Bulusheva, A. V. Gusel'nikov, V. L. Kuznetsov, Y. V. Butenko, *Carbon* **2004**, 42, 1099.  
[23] S. W. Lee, S. S. Lee, E.-H. Yang, *Nanoscale Res. Lett.* **2009**, 4, 1218.  
[24] W. Wang, X. Qin, N. Xu, Z. Li, *J. Appl. Phys.* **2011**, 109, 044304.  
[25] S. Santandrea, F. Giubileo, V. Grossi, S. Santucci, M. Passacantando, T. Schroeder, G. Lupina, A. Di Bartolomeo, *Appl. Phys. Lett.* **2011**, 98, 163109.  
[26] W. A. De Heer, A. Chatelain, D. Ugarte, *Science* **1995**, 270, 1179.  
[27] L. A. Chernozatonskii, Y. V. Gulyaev, Z. J. Kosakovskaja, N. I. Sinityn, G. V. Torgashov, Y. F. Zakharchenko, E. A. Fedorov, V. P. Val'chuk, *Chem. Phys. Lett.* **1995**, 233, 63.  
[28] A. A. Kuznetsov, S. B. Lee, M. Zhang, R. H. Baughman, A. A. Zakhidov, *Carbon* **2010**, 48, 41.